

Divergent Pressure Response of Superconductivity in Sc_6MTe_2 ($M = \text{Fe, Ru and Ir}$)

J. N. Graham,^{1,*} S.S. Islam,¹ K. Yuchi,² P. Král,¹ O. Gerguri,¹ S. Huber,^{1,3} J. Chang,³ R. Khasanov,¹ Y. Okamoto,² and Z. Guguchia^{1,†}

¹*PSI Center for Neutron and Muon Sciences CNM, 5232 Villigen PSI, Switzerland*

²*Institute for Solid State Physics, University of Tokyo, Kashiwa, Chiba 277-8581, Japan*

³*Physik-Institut, Universität Zürich, Winterthurerstrasse 190, CH-8057 Zürich, Switzerland*

(Dated: January 23, 2026)

Identifying and understanding non-BCS superconductivity remains a central challenge in condensed-matter physics. Here we focus on the Sc_6MTe_2 family ($M = d$ -electron metal), which provides a unique platform of isostructural compounds exhibiting superconductivity across $3d$, $4d$, and $5d$ systems. Using hydrostatic pressure as an additional tuning parameter, muon-spin rotation (μSR) and AC susceptibility measurements uncover strongly contrasting pressure responses of superconductivity across the Sc_6MTe_2 series. The superconducting transition temperature, T_C decreases under pressure in the $3d$ Fe-based compound but increases for the $4d$ Ru- and $5d$ Ir-based systems, with the Ru compound showing the largest enhancement of nearly 50 % within 2 GPa. The superfluid density exhibits similarly distinct pressure dependences, remaining nearly pressure independent for Fe while decreasing with increasing pressure for Ru and Ir. This suggests fundamentally different correlations between T_C and the superfluid density. Together, these results indicate that superconductivity emerging from strongly correlated and spin-orbit-dominated regimes in Sc_6MTe_2 is likely governed by different microscopic mechanisms and offer a useful experimental basis for future microscopic theoretical studies.

I. INTRODUCTION

The ability to design materials with specific properties is a compelling challenge in modern materials research. To enable such design, systematic studies across isostructural compounds are first required to understand how to manipulate physical characteristics with the chemistry toolkit. Electron correlations are widely regarded as a key ingredient for unconventional superconductivity and are realised in a broad class of correlated materials, including high- T_C cuprates [1–6], Fe-based superconductors [7–9], heavy-fermion systems [10], Sr_2RuO_4 [11, 12], kagome $AV_3\text{Sb}_5$ ($A=\text{K, Rb, Cs}$) compounds [13–19], and the nickelates [20–22]. Despite these numerous examples, it remains unclear which specific combinations of d -electron metals and crystal structures give rise to unconventional superconducting ground states. Spin-orbit coupling represents another central ingredient in quantum materials [23], capable of stabilizing unconventional superconducting phases. Contributions from electron-lattice interactions [24] have also been discussed. The ability to tune, via chemical substitution within an isostructural family and across different d -electron metals, involves balancing electron correlations, lattice effects, and spin-orbit coupling and therefore is a powerful route to systematically explore unconventional superconductivity. The case for such studies on d -electron superconductors was lacking until relatively recently with the discovery of the Sc_6MTe_2 [25] compounds.

The Sc_6MTe_2 compounds all adopt the $P\bar{6}2m$ structure without inversion symmetry and do not undergo a structural phase transition between 1.5 K to 450 K [25–28]. The structure is comprised of Sc atoms in a distorted trigonal prismatic environment surrounding a d -electron metal. These Sc_6M clusters are then connected in one-dimensional chains along the c -axis, with each chain lying at the centre of a hexagonal Te net. This structure is robust to chemical substitution from $3d$ to $5d$ systems, and recently superconductivity was found in nearly all compositions [25]. As such, this structural consistency makes the Sc_6MTe_2 compounds an ideal family to study how superconductivity evolves across varying strengths of spin-orbit coupling and electron correlations of d -electron metals.

Initially, it may be surprising the family displays superconductivity at all, given that many d -electron metals are more usually associated with magnetism. In this regard, the chemical structure is not only important from a systematics standpoint, but also the large difference in electronegativity which means that the Sc atoms donate lots of electrons to the M atoms, filling their outer shells and dramatically suppressing the magnetism [29]. Furthermore, the lack of inversion symmetry allows for more unconventional Cooper pairing mechanisms to form beyond Bardeen-Cooper-Schrieffer (BCS) theory [30, 31], as found in other non-centrosymmetric compounds like CePt_3Si [32, 33] and La_7Ir_3 [34–36]. In the Sc_6MTe_2 family, superconductivity was found to be highest for the $3d$ systems ($\text{Sc}_6\text{FeTe}_2 = 4.7$ K), with systematic variation according to their atomic number, but lower, around 2 K for $4d$ and $5d$ systems [25]. The higher T_C of the Fe compound is thought to be due to its strong electron-phonon coupling, as demonstrated by low frequency vibrations associated with Rattling phonons as presented in an *ab*

* jennifer.graham@psi.ch

† zurab.guguchia@psi.ch

initio study [29], higher than expected Sommerfeld coefficients [25], and the specific heat capacity well exceeding the weak coupling expected from BCS superconductors [25, 37]. Additionally, evidence for unconventional superconductivity in the Fe, Ru and Ir Sc_6MTe_2 compounds lies in their upper critical fields exceeding the Pauli limit [25], and from muon spin rotation/relaxation (μSR) studies which found very dilute superfluid densities, exceptionally long London penetration depths (> 1000 nm) for Sc_6RuTe_2 and Sc_6IrTe_2 , and a slight paramagnetic shift of the internal field for Sc_6IrTe_2 [28]. μSR has proposed all Sc_6MTe_2 ($M = \text{Fe, Ru, Ir}$) compounds have nodeless pairing symmetries with Sc_6FeTe_2 having two gaps [28], however NMR found a power law dependence for Sc_6RuTe_2 indicating an anisotropic gap structure [37]. Another essential feature of unconventional superconductivity is a competing or co-operative phase that may exist orders of magnitude above T_C in the normal state. The μSR study, in combination with neutron diffraction and magnetic susceptibility, found evidence that each Sc_6MTe_2 ($M = \text{Fe, Ru, Ir}$) compound has such a state, is likely magnetic in origin for Sc_6FeTe_2 , and remains unknown for Sc_6RuTe_2 and Sc_6IrTe_2 , but the studies have excluded magnetic and structural origins [28].

The delicate interplay of superconducting and normal states has been used as an advantage in leveraging superconducting properties in the past. For example, it was found in the kagome based AV_3Sb_5 ($A = \text{K, Rb, Cs}$) systems that following the complete suppression of charge order using hydrostatic pressure, superconductivity could be maximised and saturated at over 3-4 times their ambient pressure values [38–42]. A similar effect has also been seen in LaRu_3Si_2 [43, 44], 6R-TaS₂ [45, 46] and $\text{YBa}_2\text{Cu}_3\text{O}_7$ [47, 48]. However, the question still remains how the interplay of competing orders in the Sc_6MTe_2 series impacts the superconducting ground state, and to what effect spin-orbit coupling and electron correlations play in these matters. Therefore, in this article we present a highly systematic study using μSR and AC susceptibility under hydrostatic pressure to elucidate the pressure dependence of the Sc_6MTe_2 compounds. Our results reveal strikingly divergent behaviours of the superconducting transition temperature, T_C , the superfluid density, and their mutual correlation across the Sc_6MTe_2 series. Among the compounds studied, the 4d system Sc_6RuTe_2 exhibits the strongest sensitivity to applied pressure. These findings demonstrate that the pressure response of superconductivity is strongly governed by the choice of transition metal and the interplay between electronic correlations and spin-orbit coupling, providing important guidance for the development of a microscopic theory of superconductivity in Sc_6MTe_2 .

II. SUPERCONDUCTING STATE

AC susceptibility and μSR measurements were performed on arc-melted samples of Sc_6MTe_2 ($M = \text{Fe, Ru,}$

P (GPa)	0	1.1	1.7
$\lambda^{-2}(T = 0 \text{ K})(\mu\text{m}^{-2})$	5.44(5)	5.66(5)	5.74(5)
$\lambda(T > 0 \text{ K})(\text{nm})$	429	420	418
T_C (K)	4.57(6)	4.16(5)	3.79(4)
Δ (meV)	0.98(3)	0.82(2)	0.77(2)

TABLE I. Summary of superconducting gap structure parameters under pressure for Sc_6FeTe_2 . All the data were fit with a single nodeless *s*-wave model. λ is the London penetration depth, T_C is the critical superconducting temperature and Δ is the size of the gap.

Ir) under hydrostatic pressure up to 2.1 GPa, as summarised in Fig. 1. Firstly, we will examine the divergent behaviour of the critical temperature, T_C with pressure. Figure 1a shows the response of Sc_6FeTe_2 with pressure, where T_C decreases by about 1 K between ambient and the highest applied pressure. It should be noted the full transition at 0 GPa was not able to be fully measured due to technical limitations of the cryostat, however, this ambient pressure transition was verified for this sample via other methods (resistivity and DC susceptibility) [25]. In contrast, Sc_6RuTe_2 and Sc_6IrTe_2 (Fig. 1b and c, respectively) both have an overall increase in T_C with pressure, as well as a change in the magnitude of the diamagnetic response. Intriguingly, although Sc_6RuTe_2 and Sc_6IrTe_2 have nearly identical superconducting properties in ambient conditions [28], they have very different sensitivities to pressure, with the T_C of Sc_6RuTe_2 increasing by over 50 % within 2 GPa of applied pressure.

To explore the microscopic properties of the superconductivity, μSR measurements under pressure were performed on each of the samples and are summarised in Fig. 1d - f. The Sc_6FeTe_2 sample has a clear suppression of T_C , concomitant with the AC susceptibility, but the superfluid density stays nearly unchanged. An analysis of the superconducting gap structure was performed according to the supplemental material (SM), where each pressure was fit with a single nodeless *s*-wave model, and the results are summarised in Table I. This is different from the analysis at ambient pressure in Ref. [28], where the Sc_6FeTe_2 sample was best fit with a double nodeless gap, however, this discrepancy is likely due to the additional background from the pressure cell which makes resolving subtle changes, like a small secondary gap, challenging. Nevertheless, the analysis shows the London penetration depth is stable over the whole pressure range, but the size of the superconducting gap decreases by about 30 %.

The analysis and interpretation of the Sc_6RuTe_2 and Sc_6IrTe_2 compounds is different to Sc_6FeTe_2 . Firstly, technically the μSR signal is much harder to isolate in these compounds due to the much weaker superfluid density in ambient conditions [28] which is further diluted from the additional background of the pressure cell, the reduction of T_C and the limited temperature range of the instrument ($T_{\min} = 300$ mK). Therefore, we offer only a qualitative discussion of the superconducting gap structure. To isolate the magnetic signal, we performed a

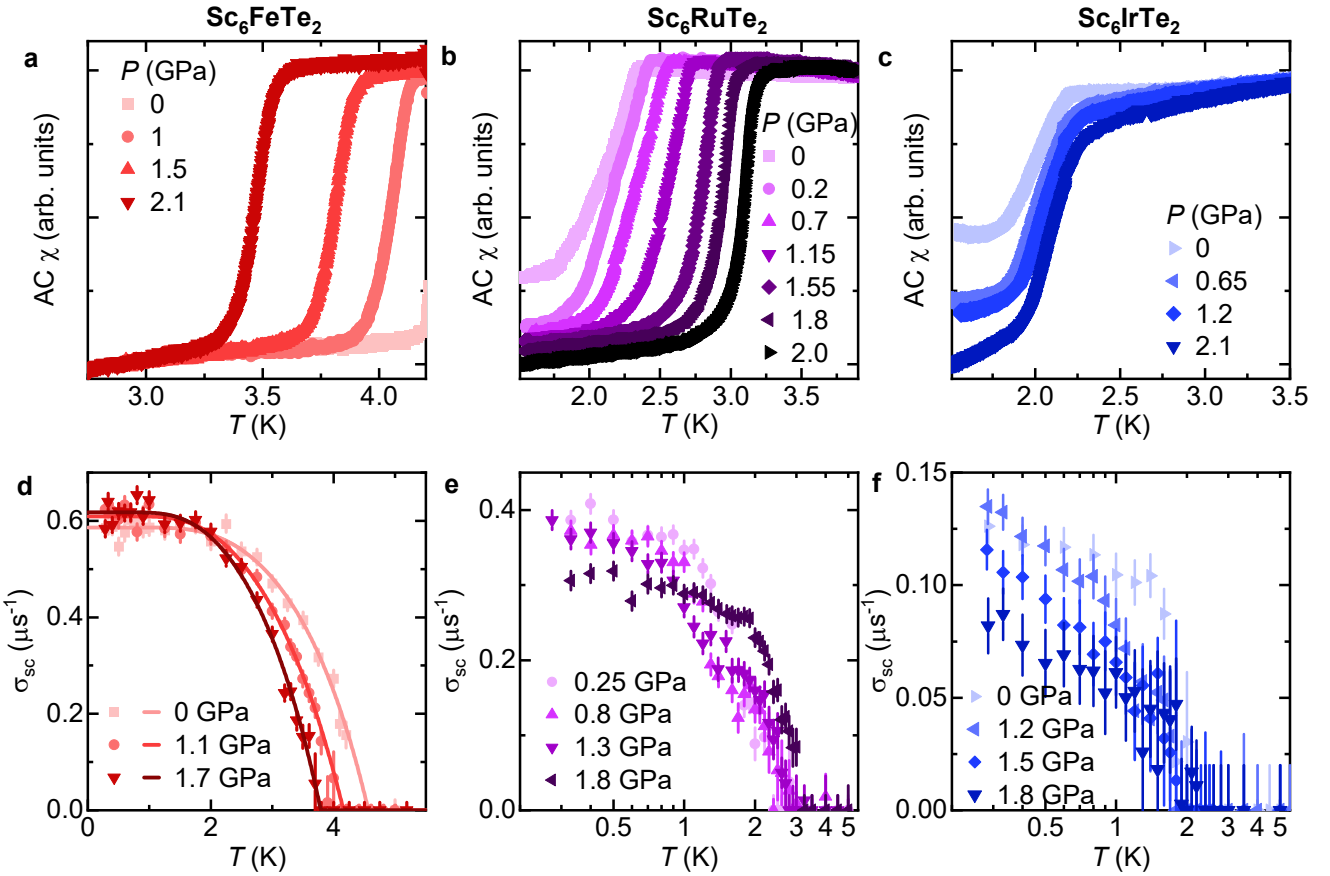


FIG. 1. **Summary of AC susceptibility and μ SR measurements under pressure on the Sc_6MTe_2 ($M = \text{Fe}, \text{Ru}, \text{Ir}$) compounds.** AC susceptibility measurements under various applied pressures up to ~ 2.1 GPa for **a** Sc_6FeTe_2 , **b** Sc_6RuTe_2 , and **c** Sc_6IrTe_2 . μ SR measurements under various applied pressures up to 1.8 GPa for **d** Sc_6FeTe_2 , **e** Sc_6RuTe_2 , and **f** Sc_6IrTe_2 . Fits of a nodeless s -wave superconducting gap structure are shown for Sc_6FeTe_2 by the solid lines in **d**. μ SR data are shown on a log-scale for Sc_6RuTe_2 (**e**) and Sc_6IrTe_2 (**f**) due to the limited temperature range.

background subtraction of the pressure cell as described in the SM. The critical temperature, T_C , is difficult to precisely determine due to the scattering of points but has already been verified through AC susceptibility measurements, and the μ SR results have a similar increase. As a result, we have put the μ SR data on a log-scale to emphasise the evolution of the superfluid density at low temperatures. Both Sc_6RuTe_2 and Sc_6IrTe_2 appear to be consistent with fully gapped behaviour within the accessible temperature range. Intriguingly though, in contrast to Sc_6FeTe_2 , both Sc_6RuTe_2 and Sc_6IrTe_2 have a reduction in their superfluid density with pressure. This is opposite from what was expected in the AC susceptibility measurements, where the magnitude of the curve increased with pressure. However, the AC magnitude is not geometry corrected and can be influenced by coil position and demagnetisation, therefore no direct comparison to superfluid density should be made.

III. NORMAL STATE

Since other studies have shown that suppressing the normal state via pressure can increase the superconducting properties or vice versa, we have explored how the normal state of the Sc_6MTe_2 ($M = \text{Fe}, \text{Ru}, \text{Ir}$) compounds responds to pressure. As a reminder, a previous μ SR study identified large increases/broadening in the normal state relaxation at $T^* = 120$ K for Sc_6FeTe_2 , 260 K for Sc_6RuTe_2 and 390 K for Sc_6IrTe_2 , which were associated with phase transitions in the normal state [28]. Sc_6FeTe_2 is the only compound we can measure the normal state of under pressure due to the Sc_6IrTe_2 transition being outside the temperature range of the cryostat (5 - 300 K), and the non-linear dependence of the pressure cell contribution at high temperatures makes interpreting data near room temperature challenging (Sc_6RuTe_2). The evolution of the normal state with pressure for Sc_6FeTe_2 is shown in Fig. 2. The data were

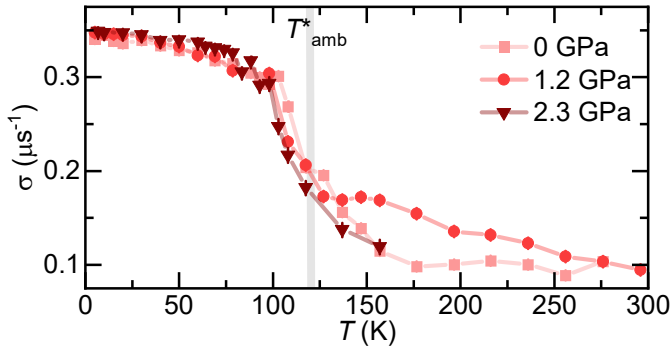


FIG. 2. **Evolution of T^* transition in the normal state of Sc_6FeTe_2 .** The change in relaxation rate, indicating a phase transition (T^*), does not change with pressure. The feature is slightly broadened from the transition determined in ambient conditions (T^*_{amb} [28]) which is likely due to the pressure cell subtraction.

fit with a Gaussian Kubo-Toyabe function multiplied by a simple exponential (Eq. 3 in SM). This is the same model used for the analysis of the ambient pressure data in Ref. [28]. The ambient pressure measurement matches well the results presented in Ref. [28], though the transition is slightly broadened. With the application of pressure, no significant change in the normal state transition is seen, despite the clear decrease in T_C over the same pressure range.

IV. DISCUSSION

Taken together, this complementary set of μ SR and AC susceptibility measurements demonstrates that the pressure response of the superconducting properties in the family Sc_6MTe_2 ($M = \text{Fe}, \text{Ru}, \text{Ir}$) depends strongly on the choice of transition metal, reflecting a crossover from dominant electronic correlations in the Fe-based compound to strong spin-orbit coupling in the Ir-based system. The main findings of this study can be summarised as follows:

(1) The critical temperature, T_C , has divergent behaviour with pressure as summarised in Fig. 3a. Figure 3a shows the change of T_C relative to its ambient pressure value. Here, it can clearly be seen that T_C for the Fe sample decreases, whereas T_C for the Ru and Ir samples increase with pressure. Overall Sc_6RuTe_2 is the most sensitive to pressure, increasing by 50 % within 2 GPa, followed by an overall change of 20 % for Sc_6FeTe_2 and less than 5 % for Sc_6IrTe_2 . The enhancement of T_C observed in both the Ir- and Ru-based compounds is particularly noteworthy, as conventional BCS superconductors typically exhibit a suppression of T_C under pressure. This behaviour suggests that applying higher pressures may further enhance T_C , naturally raising the question of whether the transition temperature will continue to increase, eventually saturate, or evolve into a dome-shaped

pressure dependence. These findings strongly motivate future experiments extending to significantly higher pressures than those explored in the present study.

(2) Besides T_C , the superfluid density is a fundamental superconducting parameter that also exhibits distinctly different pressure responses across the three compounds (Fig. 3b). In Sc_6FeTe_2 the superfluid density remains essentially unchanged under pressure despite a clear suppression of T_C . In contrast, for both Sc_6RuTe_2 and Sc_6IrTe_2 the superfluid density decreases with increasing pressure while T_C is simultaneously enhanced, with the Ru-based compound again displaying the strongest pressure sensitivity. These contrasting trends demonstrate that the correlation between T_C and superfluid density differs fundamentally among the three systems. The relationship between T_C and the superfluid density is widely regarded as a hallmark of unconventional superconductivity, and our results clearly place the Sc_6MTe_2 family within this class. Remarkably, however, the nature of this correlation depends strongly on whether superconductivity is governed by $3d$, $4d$, or $5d$ electrons. In comparison to other superconductors, the cuprates have the well-known Uemura [3] relation which establishes a linear scaling between T_C and the superfluid density in the underdoped regime, while near optimal doping the superfluid density increases with little change in T_C . Upon further overdoping, both quantities decrease, giving rise to the so-called “boomerang effect”[49]. This boomerang behaviour has long challenged simple theoretical descriptions of high- T_C superconductivity and has been attributed to several mechanisms, including strong phase fluctuations, intrinsic disorder or inhomogeneity, and competition or coexistence with other ordered states such as charge-density waves. In the case of Sc_6MTe_2 the three distinct T_C –superfluid density correlations qualitatively resembles the behaviour observed in the optimally doped and overdoped regimes of cuprates [49], highlighting a complex interplay between electronic correlations and spin-orbit coupling that evolves systematically from $3d$ to $5d$ systems. This parallel between the cuprates and Sc_6MTe_2 is highly encouraging and provides a valuable framework for theory, underscoring the importance of a microscopic understanding of phase fluctuations, quantum criticality, and anharmonic electron-lattice interactions in shaping the relationship between T_C and the superfluid density.

(3) The normal state transition, T^* for Sc_6FeTe_2 does not change with pressure (Fig. 2). This indicates that the observed changes in the superconducting properties are not directly linked to modifications of the normal-state behaviour. Instead, it suggests that distinct electronic states are involved in the formation of superconductivity and the normal-state transition. This behaviour differs from the cooperative or competitive interplay commonly observed between superconductivity and normal-state transitions, such as charge order or magnetism, in many other superconducting systems such as LaRu_3Si_2 [43, 44], $6\text{R}-\text{TaS}_2$ [45, 46], $\text{La}_{2-x}\text{Ba}_x\text{CuO}_4$ [50]

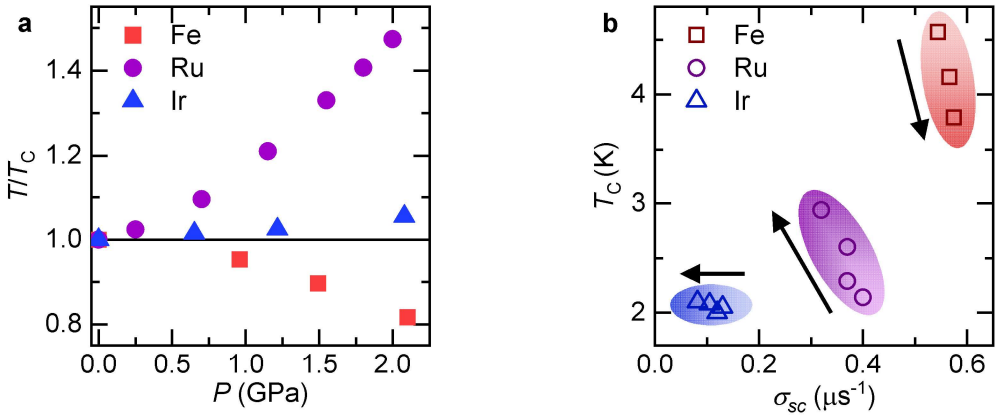


FIG. 3. Summary of pressure response of the Sc_6MTe_2 ($M = \text{Fe, Ru, Ir}$) compounds. **a** Relative change of T_C of each Sc_6MTe_2 ($M = \text{Fe, Ru, Ir}$) compound with pressure. T_C is normalised to the ambient pressure value to put all compounds on the same scale. Sc_6RuTe_2 has overall the largest change with pressure. **b** Relationship between T_C and superfluid density, σ_{sc} where all three compounds show contrasting responses with pressure. Arrows and coloured ovals (light to dark) denote increasing hydrostatic pressure.

and $\text{YBa}_2\text{Cu}_3\text{O}_7$ [47, 48]. The pressure effect between the normal state properties of Sc_6RuTe_2 and Sc_6IrTe_2 and superconductivity could not be explored in this study due to technical limitations of the cryostat and the pressure cell setup. However, earlier work found that the origin of these T^* transitions were different for Sc_6FeTe_2 and $\text{Sc}_6(\text{Ru/Ir})\text{Te}_2$ (magnetic and non-magnetic/structural, respectively). Therefore, one area that should be explored is firstly what is the origin of the T^* transition for $\text{Sc}_6(\text{Ru/Ir})\text{Te}_2$, and then is this why the compounds have contrasting responses to pressure in the superconducting state? Measurements such as ARPES, high intensity X-ray diffraction or RIXS are suitable techniques to explore the first question, once single-crystal samples of the Sc_6MTe_2 family are available.

V. CONCLUSION AND OUTLOOK

In conclusion, these results reveal intriguing divergent behaviours of how pressure and chemical tuning can impact the physics of three new d -electron based superconductors Sc_6MTe_2 ($M = \text{Fe, Ir, Ru}$). In the first instance, it is notable that the superconductor with the optimal T_C among three compounds in ambient conditions, Sc_6FeTe_2 , is destroyed with the application of pressure. In contrast, Sc_6RuTe_2 and Sc_6IrTe_2 exhibit superconducting transition temperatures that are approximately a factor of two lower than that of Sc_6FeTe_2 under ambient conditions, but their superconductivity is enhanced upon the application of pressure. Most curiously, is that the sensitivity of these two systems to pressure is very different, despite their nearly identical behaviour in ambient conditions. Ultimately, the physics of these systems appears to be governed by the interplay between electron correlations and spin-orbit coupling, yet how these effects manifest in d -electron superconductors remains an

open question. This motivates further theoretical work to elucidate how d -electron metallic states set the balance between electron correlations and spin-orbit coupling, how these interactions evolve under pressure, and the role of electron-lattice coupling. Experimentally, future studies should focus on the influence of the normal state on superconductivity in the Sc_6MTe_2 compounds and on extending the accessible pressure range to track the evolution of T_C . Understanding the distinct responses of each system will be essential for developing a unifying framework for non-BCS superconductivity in d -electron materials.

VI. METHODS

AC Susceptibility

AC susceptibility data were collected using an in-house glass cryostat system at the Paul Scherrer Institute, Villigen, Switzerland. Arc melted pellet samples were cut up to fit within the pressure chamber of a double wall MP35N/MP35N piston cell. A small amount of Daphne 7373 oil was used as the pressure medium. This cryostat setup has a maximum temperature of 4.2 K, therefore the full transition of Sc_6FeTe_2 at 0 GPa was not able to be fully measured, however, this ambient pressure transition was verified for this sample via other methods (resistivity and DC susceptibility) [25]. The pressure was determined by tracking the superconducting transition of indium against a reference indium outside the pressure cell, both of which were removed from the susceptibility curves for clarity. The absolute value of the susceptibility of each sample was artificially altered to account for differences in the coil position, but the magnitude of each curve was not corrected. This method was also used to determine the applied pressure for the μSR experiments

where the sample was loaded into a MP35N/CuBe pressure cell.

μ SR Experiments

A muon spin rotation/relaxation (μ SR) experiment consists of a beam of nearly 100 % spin polarised muons, μ^+ , which are implanted into the sample, one muon at a time. These positively charged muons stop, due to thermal stabilisation, at interstitial lattice sites in the crystal. The muon then precesses at a frequency proportional to the local internal magnetic field, B_μ , before decaying into a positron which is preferentially emitted in the direction of the muon spin, which is then detected.

Experimental details

Transverse-field (TF) and zero-field (ZF) μ SR experiments under pressure were conducted at the high pressure spectrometer, GPD [51] at the Swiss Muon Source (S μ S), Paul Scherrer Institute, Villigen, Switzerland. Arc melted pellet samples were cut up/crushed to fit within the pressure chamber of a double wall CuBe/MP35N piston cell. The double wall cell is specifically designed for high-pressure measurements and can reach applied pressures of 2.3 GPa at room temperature. The CuBe/MP35N alloy was chosen because it has a lower background for μ SR experiments, which was required due to the very dilute superfluid signal. Daphne 7373 oil was used as a pressure medium. For the measurements in the superconducting state, a Variox He-4 cryostat with a He-3 insert was used to control the temperature, allowing temperatures of 300 mK. A TF of 30 mT was applied to Sc₆FeTe₂, and 20 mT applied to Sc₆RuTe₂ and Sc₆IrTe₂. These TFs were chosen to match the ambient pressure TFs applied in Ref. [28]. The field was applied at 10 K, and the samples cooled in field, to access the vortex state. For the ZF measurements in the normal state, a Janis cryostat, with a temperature range of 5 - 300 K, was used to control the temperature. Measurements of the pressure cell background were made by lowering the muon momentum to 98 MeV/c, so that the majority of the muons stop within the cell. These measurements were only performed under an applied TF of 20 mT between 300 mK and 5 K.

Data reduction and analysis

The superfluid density can be accurately measured by the μ SR technique from the evolution of the muon spin depolarisation rate, σ_{tot} as a function of temperature. This depolarisation rate is proportional to the width of the internal field experienced by the muon, which for a superconductor is comprised of two components, a superconducting, σ_{sc} and nuclear magnetic dipolar, σ_{nm} con-

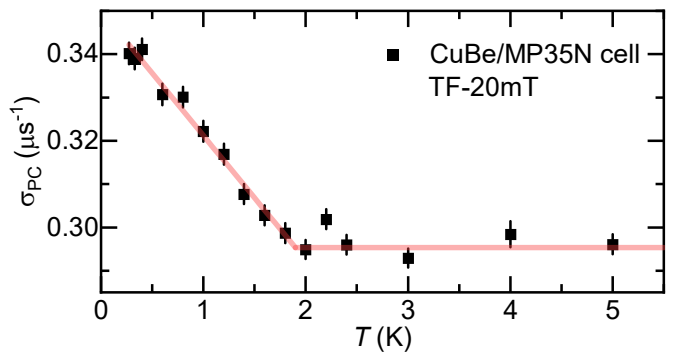


FIG. 4. The temperature dependence of the relaxation rate of the CuBe/MP35N pressure cell with the sample inside is shown. The measurements were performed in a 20 mT applied transverse field at a muon momentum of 98 MeV/c, for which the majority of muons stop in the pressure cell. The relaxation rate exhibits a non-linear temperature dependence, with only a very weak increase below 2 K attributable to the influence of the superconducting sample.

tribution ($\sigma_{\text{tot}}^2 = \sigma_{\text{sc}}^2 + \sigma_{\text{nm}}^2$). For measurements under hydrostatic pressure there is an additional contribution from the muons that stop within the pressure cell, and can thus be considered as an additional background. This is particularly problematic for Sc₆RuTe₂ and Sc₆IrTe₂, which from our μ SR measurements in ambient conditions had maximal σ_{sc} values of 0.15 μs^{-1} and 0.1 μs^{-1} , respectively [28]. To address this issue, we performed an additional measurement at 20 mT using a reduced muon momentum, such that the majority of muons stop in the pressure cell. The sample remains inside the cell and therefore still influences the pressure-cell signal, which is precisely what we aim to probe, as this configuration allows us to directly characterize the pressure-cell background under the same experimental conditions as the sample measurements. The pressure cell was fit with the following function:

$$A_{\text{PC}}(t) = A_{\text{PC}} \exp \left[-\frac{1}{2} (\sigma_{\text{PC}} t^2) \right] \cos(\gamma_\mu B_{\text{PC}} t + \varphi_{\text{PC}}) \quad (1)$$

where A_{PC} is the initial asymmetry of the pressure cell, σ_{PC} is the depolarisation rate of the pressure cell, γ_μ is the gyromagnetic ratio of the muon, B_{PC} is the internal field of the pressure cell and φ_{PC} is the phase shift of the pressure cell. As shown in Fig. 4, the pressure cell exhibits a very weak increase in the relaxation rate below 2 K, which arises from the influence of the superconducting sample. Although this increase is small, given that the superfluid responses of both the Ir- and Ru-based samples are weak, we interpolate this non-linear increase (red line) and use it as the background contribution in our data reduction. The background was subtracted in quadrature from σ_{tot} for both Sc₆RuTe₂ and Sc₆IrTe₂.

The Sc₆FeTe₂, Sc₆RuTe₂ and Sc₆IrTe₂ superconduct-

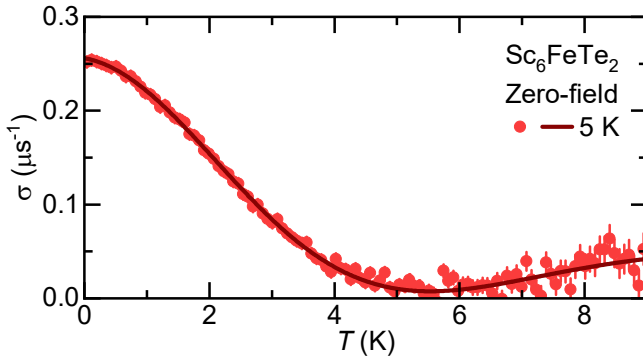


FIG. 5. Example fit of zero-field μ SR data in the normal state of Sc_6FeTe_2 at 5 K. Data were fit with Eq. 3.

ing data were fit with the following function:

$$A_{\text{TF}}(t) = A_S \exp \left[-\frac{1}{2}(\sigma_S t^2) \right] \cos(\gamma_\mu B_{\text{int},S} t + \varphi_S) + A_{\text{PC}}(t) \quad (2)$$

where A_S is the initial asymmetry of the sample, σ_S is the depolarisation rate of the sample, $B_{\text{int},S}$ is the internal field of the sample, φ_S is the phase shift of the sample and $A_{\text{PC}}(t)$ is the pressure cell contribution, as defined in Eq. 1.

Following the background subtraction, σ_{sc} can be estimated by subtracting in quadrature σ_{nm} (assumed to be constant above T_C) from the corrected σ_{tot} . σ_{sc} for each pressure is shown in Fig. 1d - f.

The normal state zero-field data of Sc_6FeTe_2 were fit with the following Gaussian Kubo-Toyabe depolarisation function multiplied by an exponential term

$$A_{\text{ZF}}^{\text{GKT}}(t) = \sum_i^n A \left[\left(\frac{1}{3} + \frac{2}{3}(1 - \sigma_i^2 t^2) \exp \left[-\frac{\sigma_i^2 t^2}{2} \right] \right) \exp(-\Gamma_i t) \right] \quad (3)$$

where σ_i and Γ_i are the muon relaxation rates. For these measurements there are two i components, a pressure cell and sample contribution. This formula is consistent with the functional form used in Ref. [28] for the ambient

pressure data. An example fit of the data at 5 K is shown in Fig. 5.

Superconducting gap structure analysis

To perform a quantitative analysis of μ SR data and determine the superconducting gap structure, the superconducting muon spin depolarisation rate, $\sigma_{\text{sc}}(T)$ in the presence of a perfect triangular vortex lattice is first related to the London penetration depth, $\lambda(T)$ by the following equation [52, 53]:

$$\frac{\sigma_{\text{sc}}(T)}{\gamma_\mu} = 0.06091 \frac{\Phi_0}{\lambda^2(T)} \quad (4)$$

where $\Phi_0 = 2.068 \times 10^{-15}$ Wb is the magnetic flux quantum. This equation is only applicable when the separation between the vortices is larger than λ . In this particular case, as per the London model, σ_{sc} becomes field independent. By analysing the temperature dependence of the magnetic penetration depth, within the local London approximation, a direct association with the superconducting gap symmetry can be made [54]:

$$\frac{\lambda^{-2}(T, \Delta_{0,i})}{\lambda^{-2}(0, \Delta_{0,i})} = 1 + \frac{1}{\pi} \int_0^{2\pi} \int_{\Delta(T, \phi)}^{\infty} \left(\frac{\delta f}{\delta E} \right) \frac{EdEd\varphi}{\sqrt{E^2 - \Delta_i(T, \varphi)^2}} \quad (5)$$

where $f = [1 + \exp(E/k_B T)]^{-1}$ is the Fermi function, φ is the angle along the Fermi surface, and $\Delta_i(T, \varphi) = \Delta_{0,i} \Gamma(T/T_C) g(\varphi)$ ($\Delta_{0,i}$ is the maximum gap value at $T = 0$). The temperature dependence of the gap is approximated by the expression, $\Gamma(T/T_C) = \tanh[1.82[1.018(T_C/T - 1)]^{0.51}]$ [55], whilst $g(\varphi)$ describes the angular dependence of the new gap and is replaced by 1 for an s -wave gap, $[1 + \cos(4\varphi)/(1 + a)]$ for an anisotropic s -wave gap, and $|\cos(2\varphi)|$ for a d -wave gap [56].

[1] K. A. Müller and J. G. Bednorz, The discovery of a class of high-temperature superconductors, *Science* **237**, 1133 (1987), <https://www.science.org/doi/pdf/10.1126/science.237.4819.1133>.

[2] B. Keimer, S. Kivelson, M. Norman, S. Uchida, and J. Zaanen, From quantum matter to high-temperature superconductivity in copper oxides, *Nature* **518**, 179 (2015).

[3] Y. Uemura, G. Luke, B. Sternlieb, J. Brewer, J. Carolan, W. Hardy, R. Kadono, J. Kempton, R. Kiefl, S. Kreitzman, *et al.*, Universal Correlations between T_c and $\frac{n_s}{m^*}$ (Carrier Density over Effective Mass) in High- T_c Cuprate Superconductors, *Physical review letters* **62**, 2317 (1989).

[4] R. L. Greene, P. R. Mandal, N. R. Poniawski, and T. Sarkar, The strange metal state of the electron-doped cuprates, *Annual Review of Condensed Matter Physics* **11**, 213 (2020).

[5] M. A. Rahman, M. Z. Rahaman, and M. N. Samsuddoha, A review on cuprate based superconducting materials including characteristics and applications, *American Journal of Physics and Applications* **3**, 39 (2015).

[6] S. M. Hayden and J. M. Tranquada, Charge correlations in cuprate superconductors, *Annual Review of Condensed Matter Physics* **15** (2023).

[7] R. M. Fernandes, A. I. Coldea, H. Ding, I. R. Fisher, P. J. Hirschfeld, and G. Kotliar, Iron pnictides and chalco-

genides: a new paradigm for superconductivity, *Nature* **601**, 35–44 (2022).

[8] I. I. Mazin, Superconductivity gets an iron boost, *Nature* **464**, 183 (2010).

[9] R. Fernandes, A. Chubukov, and J. Schmalian, What drives nematic order in iron-based superconductors?, *Nature physics* **10**, 97 (2014).

[10] G. R. Stewart, Heavy-fermion systems, *Rev. Mod. Phys.* **56**, 755 (1984).

[11] Y. Maeno, T. M. Rice, and M. Sigrist, The intriguing superconductivity of strontium ruthenate, *Physics Today* **54**, 42 (2001), https://pubs.aip.org/physicstoday/article-pdf/54/1/42/11109470/42_1_online.pdf.

[12] A. P. Mackenzie and Y. Maeno, The superconductivity of sr_2ruo_4 and the physics of spin-triplet pairing, *Reviews of Modern Physics* **75**, 657 (2003).

[13] B. R. Ortiz, S. M. L. Teicher, Y. Hu, J. L. Zuo, P. M. Sarte, E. C. Schueller, A. M. M. Abeykoon, M. J. Krogstad, S. Rosenkranz, R. Osborn, R. Seshadri, L. Balaents, J. He, and S. D. Wilson, Csv_3sb_5 : A F_2 topological kagome metal with a superconducting ground state, *Phys. Rev. Lett.* **125**, 247002 (2020).

[14] Y.-X. Jiang, J.-X. Yin, M. M. Denner, N. Shumiya, B. R. Ortiz, G. Xu, Z. Guguchia, J. He, M. S. Hossain, X. Liu, *et al.*, Unconventional chiral charge order in kagome superconductor kv_3sb_5 , *Nature materials* **20**, 1353 (2021).

[15] Y. Hu, X. Wu, B. R. Ortiz, S. Ju, X. Han, J. Ma, N. C. Plumb, M. Radovic, R. Thomale, S. D. Wilson, *et al.*, Rich nature of van hove singularities in kagome superconductor csv_3sb_5 , *Nature Communications* **13**, 2220 (2022).

[16] C. Mielke III, D. Das, J.-X. Yin, H. Liu, R. Gupta, Y.-X. Jiang, M. Medarde, X. Wu, H. C. Lei, J. Chang, *et al.*, Time-reversal symmetry-breaking charge order in a kagome superconductor, *Nature* **602**, 245 (2022).

[17] Z. Guguchia, R. Khasanov, and H. Luetkens, Unconventional charge order and superconductivity in kagome-lattice systems as seen by muon-spin rotation, *npj Quantum Materials* **8**, 41 (2023).

[18] J. N. Graham, C. Mielke III, D. Das, T. Morresi, V. Sazgari, A. Suter, T. Prokscha, H. Deng, R. Khasanov, S. D. Wilson, A. C. Salinas, M. M. Martins, Y. Zhong, K. Okazaki, Z. Wang, M. Z. Hasan, M. H. Fischer, T. Neupert, J. X. Yin, S. Sanna, H. Luetkens, Z. Salman, P. Bonfà, and Z. Guguchia, Depth-dependent study of time-reversal symmetry-breaking in the kagome superconductor a_3sb_5 , *Nature Communications* **15**, 8978 (2024).

[19] Y. Wang, H. Wu, G. T. McCandless, J. Y. Chan, and M. N. Ali, Quantum states and intertwining phases in kagome materials, *Nature Reviews Physics* **5**, 635 (2023).

[20] B. Y. Wang, K. Lee, and B. H. Goodge, Experimental Progress in Superconducting Nickelates, *Annual Review of Condensed Matter Physics* **15**, <https://doi.org/10.1146/annurev-conmatphys-032922-093307> (2024).

[21] Y. Nomura and R. Arita, Superconductivity in infinite-layer nickelates, *Reports on Progress in Physics* **85**, 052501 (2022).

[22] R. Khasanov, T. J. Hicken, D. J. Gawryluk, V. Sazgari, I. Plokikh, L. P. Sorel, M. Bartkowiak, S. Bötz, F. Lechermann, I. M. Eremin, *et al.*, Pressure-enhanced splitting of density wave transitions in $la_3ni_2o_7-\delta$, *Nature Physics* **1**, 1 (2025).

[23] W. Witczak-Krempa, G. Chen, Y. B. Kim, and L. Balents, Correlated quantum phenomena in the strong spin-orbit regime, *Annual Review of Condensed Matter Physics* **5**, 57 (2014).

[24] H. Keller, Unconventional isotope effects in cuprate superconductors, in *Superconductivity in Complex Systems: -/-*, edited by K. A. Müller and A. Bussmann-Holder (Springer Berlin Heidelberg, Berlin, Heidelberg, 2005) pp. 143–169.

[25] Y. Shinoda, Y. Okamoto, Y. Yamakawa, H. Matsumoto, D. Hirai, and K. Takenaka, Superconductivity in Ternary Scandium Telluride Sc_6MT_2 with $3d$, $4d$, and $5d$ Transition Metals, *Journal of the Physical Society of Japan* **92**, 103701 (2023).

[26] P. A. Maggard and J. D. Corbett, Sc_6MT_2 ($M = Mn$, Fe , Co , Ni): Members of the flexible Zr_6CoAl_2 -type family of compounds, *Inorganic Chemistry* **39**, 4143 (2000).

[27] L. Chen and J. D. Corbett, Synthesis, structure, and bonding of Sc_6MT_2 ($M = Ag$, Cu , Cd): Heterometal-induced polymerization of metal chains in Sc_2Te , *Inorganic chemistry* **41**, 2146 (2002).

[28] J. N. Graham, K. Yuchi, V. Sazgari, A. Doll, C. Mielke III, P. Král, O. Gerguri, S. S. Islam, V. Pomjakushin, M. L. Medarde, H. Luetkens, Y. Okamoto, and Z. Guguchia, Tailoring the Normal and Superconducting State Properties of Ternary Scandium Tellurides, Sc_6MT_2 ($M = Fe$, Ru , and Ir) Through Chemical Substitution, *Advanced Functional Materials* **25**, 2505517 (2025).

[29] M.-C. Jiang, R. Masuki, G.-Y. Guo, and R. Arita, Ab initio study on magnetism suppression, anharmonicity, rattling mode, and superconductivity in Sc_6MT_2 ($M = Fe$, Co , Ni), *Phys. Rev. B* **110**, 104505 (2024).

[30] M. H. Fischer, M. Sigrist, D. F. Agterberg, and Y. Yanase, Superconductivity and local inversion-symmetry breaking, *Annual Review of Condensed Matter Physics* **14**, 153 (2023).

[31] M. Sigrist, Introduction to unconventional superconductivity in non-centrosymmetric metals, in *AIP Conference Proceedings*, Vol. 1162 (American Institute of Physics, 2009) pp. 55–96.

[32] K. V. Samokhin, E. S. Zijlstra, and S. K. Bose, $CePt_3Si$: An unconventional superconductor without inversion center, *Physical Review B* **69**, 094514 (2004).

[33] E. Bauer, H. Kaldarar, A. Prokofiev, E. Royanian, A. Amato, J. Sereni, W. Brämer-Escamilla, and I. Bonalde, Heavy fermion superconductivity and antiferromagnetic ordering in $cept_3si$ without inversion symmetry, *Journal of the Physical Society of Japan* **76**, 051009 (2007).

[34] J. A. T. Barker, D. Singh, A. Thamizhavel, A. D. Hillier, M. R. Lees, G. Balakrishnan, D. M. Paul, and R. P. Singh, Unconventional superconductivity in La_7Ir_3 revealed by muon spin relaxation: Introducing a new family of noncentrosymmetric superconductor that breaks time-reversal symmetry, *Physical Review Letters* **115**, 267001 (2015).

[35] B. Li, C. Q. Xu, W. Zhou, W. H. Jiao, R. Sankar, F. M. Zhang, H. H. Hou, X. F. Jiang, B. Qian, B. Chen, and X. Xu, Evidence of s -wave superconductivity in the non-centrosymmetric La_7Ir_3 , *Scientific Reports* **8**, 651 (2018).

[36] D. A. Mayoh, A. D. Hillier, G. Balakrishnan, and M. R. Lees, Evidence for the coexistence of time-reversal symmetry breaking and Bardeen-Cooper-Schrieffer-like superconductivity in La_7Pd_3 , *Physical Review B* **103**,

024507 (2021).

[37] K. Doi, H. Takei, Y. Shinoda, Y. Okamoto, D. Hirai, K. Takenaka, T. Matsushita, Y. Kobayashi, and Y. Shimizu, Anisotropic superconducting gap probed by Te 125 NMR in noncentrosymmetric Sc_6MTe_2 ($M = Fe, Co$), *Physical Review B* **111**, 214502 (2025).

[38] R. Gupta, D. Das, C. H. Mielke III, Z. Guguchia, T. Shiroka, C. Baines, M. Bartkowiak, H. Luetkens, R. Khasanov, Q. Yin, Z. Tu, C. Gong, and H. Lei, Microscopic evidence for anisotropic multigap superconductivity in the CsV_3Sb_5 kagome superconductor, *npj Quantum Materials* **7**, 49 (2022).

[39] Z. Guguchia, C. Mielke III, D. Das, R. Gupta, J.-X. Yin, H. Liu, Q. Yin, M. H. Christensen, Z. Tu, C. Gong, N. Shumiya, M. Shafayat Hossain, T. Gamsakhurdashvili, M. Elender, P. Dai, A. Amato, Y. Shi, H. C. Lei, R. M. Fernandes, M. Z. Hasan, H. Luetkens, and R. Khasanov, Tunable unconventional kagome superconductivity in charge ordered RbV_3Sb_5 and KV_3Sb_5 , *Nature communications* **14**, 153 (2023).

[40] J. N. Graham, S. S. Islam, V. Sazgari, Y. Li, H. Deng, G. Janka, Y. Zhong, O. Gerguri, P. Král, A. Doll, I. Bialo, J. Chang, Z. Salman, A. Suter, T. Prokscha, Y. Yao, K. Okazaki, H. Luetkens, R. Khasanov, Z. Wang, J.-X. Yin, and Z. Guguchia, Pressure induced transition from chiral charge order to time-reversal symmetry-breaking superconducting state in Nb-doped CsV_3Sb_5 , *Communications Physics* **8**, 318 (2025).

[41] L. Zheng, Z. Wu, Y. Yang, L. Nie, M. Shan, K. Sun, D. Song, F. Yu, J. Li, D. Zhao, S. Li, B. Kang, Y. Zhou, K. Liu, Z. Xiang, J. Ying, Z. Wang, T. Wu, and X. Chen, Emergent charge order in pressurized kagome superconductor CsV_3Sb_5 , *Nature* **611**, 682 (2022).

[42] T. Neupert, M. M. Denner, J.-X. Yin, R. Thomale, and M. Z. Hasan, Charge order and superconductivity in kagome materials, *Nature Physics* **18**, 137 (2022).

[43] K. Ma, I. Plokhikh, J. N. Graham, C. Mielke III, V. Sazgari, H. Nakamura, S. S. Islam, S. Shin, P. Král, O. Gerguri, H. Luetkens, F. O. von Rohr, J. Yin, E. Pomjakushina, C. Felser, S. Nakatsui, B. Wehinger, D. J. Gawryluk, S. Medvedev, and Z. Guguchia, Correlation between the dome-shaped superconducting phase diagram, charge order, and normal-state electronic properties in $LaRu_3Si_2$, *Nature Communications* **16**, 6149 (2025).

[44] Z. Li, S. Huyan, E. C. Thompson, T. J. Slade, D. Zhang, Y. J. Ryu, W. Bi, S. L. Bud'ko, and P. C. Canfield, Superconducting dome and structural changes in $LaRu_3Si_2$ under pressure, *Physical Review B* **111**, 144505 (2025).

[45] V. Sazgari, J. N. Graham, S. S. Islam, O. Gerguri, A. Achari, J. N. Tangermann, H. Gopakumar, G. Simutis, M. Janoschek, M. Bartkowiak, R. Khasanov, H. Luetkens, F. O. von Rohr, R. R. Nair, and Z. Guguchia, Competing Quantum Orders in 6R-TaS₂: Unconventional Superconductivity, Charge Order, and an Anomalous Hall Effect phase, *arXiv preprint arXiv:2503.13944* <https://doi.org/10.48550/arXiv.2503.13944> (2025).

[46] Y. Liu, W. J. Lu, L. J. Li, X. D. Zhu, W. H. Song, R. Ang, L. S. Ling, X. Z. Liu, and Y. P. Sun, Tuning the charge density wave and superconductivity in 6R-TaS_{2-x}Se_x, *Journal of Applied Physics* **117**, <https://doi.org/10.1063/1.4919219> (2015).

[47] C. Putzke, J. Ayres, J. Buhot, S. Licciardello, N. E. Hussey, S. Friedemann, and A. Carrington, Charge order and superconductivity in underdoped $YBa_2Cu_3O_{7-\delta}$ under Pressure, *Physical Review Letters* **120**, 117002 (2018).

[48] O. Cyr-Choinière, D. LeBoeuf, S. Badoux, S. Dufour-Beauséjour, D. A. Bonn, W. N. Hardy, R. Liang, D. Graf, N. Doiron-Leyraud, and L. Taillefer, Sensitivity of T_c to pressure and magnetic field in the cuprate superconductor $YBa_2Cu_3O_y$: Evidence of charge-order suppression by pressure, *Physical Review B* **98**, 064513 (2018).

[49] C. Niedermayer, C. Bernhard, U. Binninger, H. Glückler, J. L. Tallon, E. J. Ansaldi, and J. I. Budnick, Muon spin rotation study of the correlation between T_c and n_s/m^* in overdoped $Tl_2Ba_2CuO_{6+\delta}$, *Phys. Rev. Lett.* **71**, 1764 (1993).

[50] Z. Guguchia, D. Das, C. Wang, T. Adachi, N. Kitajima, M. Elender, F. Brückner, S. Ghosh, V. Grinenko, T. Shiroka, M. Muller, C. Mudry, C. Baines, M. Bartkowiak, Y. Koike, A. Amato, J. M. Tranquada, H.-H. Klauss, C. W. Hicks, and H. Luetkens, Using uniaxial stress to probe the relationship between competing superconducting states in a cuprate with spin-stripe order, *Physical Review Letters* **125**, 097005 (2020).

[51] R. Khasanov, Perspective on muon-spin rotation/relaxation under hydrostatic pressure, *Journal of Applied Physics* **132**, <https://doi.org/10.1063/5.0119840> (2022).

[52] E. H. Brandt, Flux distribution and penetration depth measured by muon spin rotation in high- T_c superconductors, *Phys. Rev. B* **37**, 2349 (1988).

[53] E. H. Brandt, Properties of the ideal ginzburg-landau vortex lattice, *Phys. Rev. B* **68**, 054506 (2003).

[54] A. Suter and B. Wojek, Musrfit: A free platform-independent framework for μ sr data analysis, *Physics Procedia* **30**, 69 (2012), 12th International Conference on Muon Spin Rotation, Relaxation and Resonance (μ SR2011).

[55] A. Carrington and F. Manzano, Magnetic penetration depth of mgb2, *Physica C: Superconductivity* **385**, 205 (2003).

[56] M. H. Fang, H. M. Pham, B. Qian, T. J. Liu, E. K. Vehstedt, Y. Liu, L. Spinu, and Z. Q. Mao, Superconductivity close to magnetic instability in $Fe(Se_{1-x}Te_x)_{0.82}$, *Phys. Rev. B* **78**, 224503 (2008).

VII. ACKNOWLEDGMENTS

Z.G. acknowledges support from the Swiss National Science Foundation (SNSF) through SNSF Starting Grant (No. TMSGI2.211750). Y.O. and K.Y. acknowledge support from the Japan Science and Technology Agency through JST-ASPIRE (No. JPMJAP2314).

VIII. AUTHOR CONTRIBUTIONS

Z.G. conceived and supervised the project. Sample growth: K.Y. and Y.O.. High pressure AC susceptibility experiments: J.N.G., S.S.I., and Z.G.. High pressure

μ SR experiments, the corresponding analysis and discussions: J.N.G., S.S.I., P.K., O.G., R.K., and Z.G.. Figure development and writing of the paper: J.N.G. and Z.G.. All authors discussed the results, interpretation, and conclusion.

DATA AVAILABILITY

The data that support the findings of this study are available from the corresponding authors upon request.

CONFLICT OF INTEREST

The authors declare no financial/commercial conflict of interest.